Ab initio molecular dynamics simulation of liquid Al_xGe_{1-x} alloys

Songyou Wang,[1,2] C. Z. Wang,[1] Feng-Chuan Chuang,[1] James R. Morris,[3] and K. M. Ho[1]

[1]*Ames Laboratory, U.S. Department of Energy and Department of Physics and Astronomy, Iowa State University, Ames, Iowa 50011, USA*

[2]*Department of Optical Science and Engineering, State Key Laboratory of Advanced Photonic Materials and Devices, Fudan University, Shanghai 200433, People's Republic of China*

[3]*Metals and Ceramics Division, Oak Ridge National Laboratory, Oak Ridge, Tennessee 37831-6115, USA*

First-principles molecular dynamics simulations are carried out to study the structural, dynamical, and electronic properties of liquid Al_xGe_{1-x} with 0.0, 0.2, 0.4, 0.6, 0.8, and 1.0 of aluminum concentration. The concentration dependence of static structure factors, pair correlation functions, diffusion constants, and electronic density-of-states at temperature of 1250 K are investigated. The structural properties obtained from the simulations are in good agreement with neutron scattering experimental results.

I. INTRODUCTION

The study of liquid metals and alloys has drawn considerable attention recently, in particular due to the feasibility of carrying out *ab initio* molecular dynamics simulations for these systems.[1–3] In *ab initio* molecular dynamics simulations, the electronic structure and total energy are evaluated using the density-functional theory and the corresponding forces are used to move the ions according to classical molecular dynamics. Using this approach it is possible to calculate both the atomic and electronic structure consistently and to study how changes in one are correlated with changes in the other. In recent years, the thermodynamic and transport properties of a variety of liquid metals and alloys have been studied by this method.[4–7] Many interesting materials, such as Ga_xAs_{1-x}, Ga_xGe_{1-x}, FeS, and $GeSe_2$ have been investigated. Results from *ab initio* molecular dynamics simulations are found to be in good agreement with experiments.

Aluminum and germanium are two important materials and have very different bonding properties. The structures of Al and Ge in liquid state have been measured by x-ray diffraction and neutron scattering.[8] While Al is a face-centered-cubic metal and Ge is a tetrahedral semiconductor in the crystalline phase, both elements in the liquid state are metallic with coordination numbers of 11.5 and 6.8 for Al and Ge, respectively.[9] Recently, the structures, electronic, and dynamical properties of the liquid Al_xGe_{1-x} alloys have attracted a lot of interest. The structure factors of the liquid Al_xGe_{1-x} alloys with x ranging from 0.2 to 0.8 have been measured by Grosdidier and Gasser[10,11] using neutron scattering at 1250 K. They found that the pair correlation functions of the liquid Al_xGe_{1-x} alloys have similar shape, but the intensity of the first peak increased with increasing the concentration of Al. The electronic density of states of Al_xGe_{1-x} alloys both in the liquid and in the amorphous state has been measured by Gampp *et al.*[12] using the photoelectron spectroscopy. They suggested that there is a minimum in the electronic density-of-state at the Fermi energy which is absent in the pure liquid alloy constituents.

Despite a lot experimental efforts, the atomic structures and the relationship between the structures and properties of

the liquids are still not well understood. Knowledge about the liquid structures and properties from atomistic simulations is therefore desirable. In this paper, we describe a numerical study of Al_xGe_{1-x} liquids over a range of concentrations, using *ab initio* molecular dynamics simulations. The paper is organized as follows: A brief description of the calculation method is given in Sec. II. The results of the simulations are presented in Sec. III, followed by a summary in Sec. IV.

II. COMPUTATION METHOD

Our simulations were carried out using the Vienna *ab initio* simulation package.[13] The system consists of 50 atoms at constant volume in a cubic box with the periodic boundary conditions. The molecular dynamics simulations were carried out at the temperature of 1250 K which is above the melting point of the system. We considered four concentrations of Al_xGe_{1-x} alloys with $x=0.2$, 0.4, 0.6, and 0.8. The liquid state of pure Al and Ge were also simulated for the purpose of comparison. The atomic number densities at the four concentrations are determined by a linear combination of the densities of pure liquid Al (ρ_1) and Ge (ρ_2):

$$\rho = c_1\rho_1 + c_2\rho_2, \qquad (1)$$

where c_1 and c_2 are concentrations of Al and Ge, respectively. Using the mass density $d_i = a_i - b_i(T - T_{Mi})$ (where T_{Mi} is the melting temperature of ith pure metal) from Crawley,[14] the atomic number densities ρ_1 and ρ_2 of the pure Al and Ge liquids are chosen to be 0.046 28 and 0.051 36 atom/$Å^3$, respectively, at the temperature of 1250 K. We use linear combination of the density of liquid Al and Ge as the densities of liquid Al_xGe_{1-x} alloys because no experimental values are available in the literature. A similar linear combination scheme has also been used in Ref. 10. It should be noted that this is an approximation and the realistic densities will deviate from the linear combination values when intermixing is presented in the liquids. In order to see how sensitive is the structure and properties of the liquid alloys to the density, we have performed simulations for liquid $Al_{0.6}Ge_{0.4}$ at three dif-

ferent densities (0.048 82, 0.049 33, 0.049 84 atom/Å^3, where 0.049 33 is the value from linear combination scheme). Liquid Al$_{0.6}$Ge$_{0.4}$ is chosen because intermixing is strong in this concentration and the deviation of the density from the linear combination value will be more pronounce. The simulation results show that the structure of the liquids is not sensitive to the small density changes. The changes in the pair correlation function and structure factor are very small. However, the diffusion constant does have noticeable changes. Therefore, the uncertainty in the density will cause some error in the diffusion constant as will be shown in Sec. III.

For a given ionic configuration, the total energy of the system is calculated using first-principles density functional formalism. The force on each ion is calculated using the Hellmann-Feynman theorem. Newton's equations of motion are integrated numerically for the ions, using a time step of 3.0 fs. We used the canonical ensemble where the ions temperature was controlled using the Nose-Hoover thermostat.[15] The density functional calculations are performed using a plane-wave pseudopotential representation, with ultrasoft pseudopotentials[13,16] for both Al and Ge species and with a plane-wave energy cutoff of 140 eV. The Γ-point sampling is used for the supercell Brillouin zone. Our simulations were performed using the local-density approximation for the exchange correlation energy.

We start the simulations with the 50 atoms in random positions in the cubic supercell. This starting configuration is allowed to iterate for 2000 time step (6 ps) at a temperature of 1600 K. Then the system is cooled down to 1250 K at a uniform cooling rate for about 1.5 ps. The simulations were further carried out for another 2000 time steps (6 ps) to collect the configurations for statistical analysis of the structures and properties of the liquid.

III. RESULTS AND DISCUSSION

A. Structural properties

Pair correlation function $g(r)$ is an important quantity to characterize liquid structures, which is defined as follows:

$$g(r) = \rho^{-2} \left\langle \sum_i \sum_{j \neq i} \delta(\mathbf{r}_i) \delta(\mathbf{r}_j - \mathbf{r}) \right\rangle. \quad (2)$$

This function gives the probability of finding a pair of atoms at a distance r apart. Using the atomic coordinates from the molecular dynamics simulations, the total pair correlation function $g(r)$ are calculated according to Eq. (2) for liquid Al$_x$Ge$_{1-x}$ at the Al concentration of $x = 0.2$, 0.4, 0.6, and 0.8 and at the temperature of 1250 K. The partial pair correlation functions $g_{\text{Al-Ge}}(r)$, $g_{\text{Al-Al}}(r)$, and $g_{\text{Ge-Ge}}(r)$ can also be calculated when the density in Eq. (2) is set to be the corresponding partial density $\rho_{ij} = \rho\sqrt{c_i c_j}$ where ρ is the density of the system, i and j denote the elements in the alloy, and c_i and c_j are their concentrations. The results are presented in Fig. 1.

As can be seen from the Fig. 1(a), the first peak position of the total pair correlation function is shifted from 2.66 to 2.74 Å with increasing the concentration of Al. The height of the peaks also increases with increasing Al concentration.
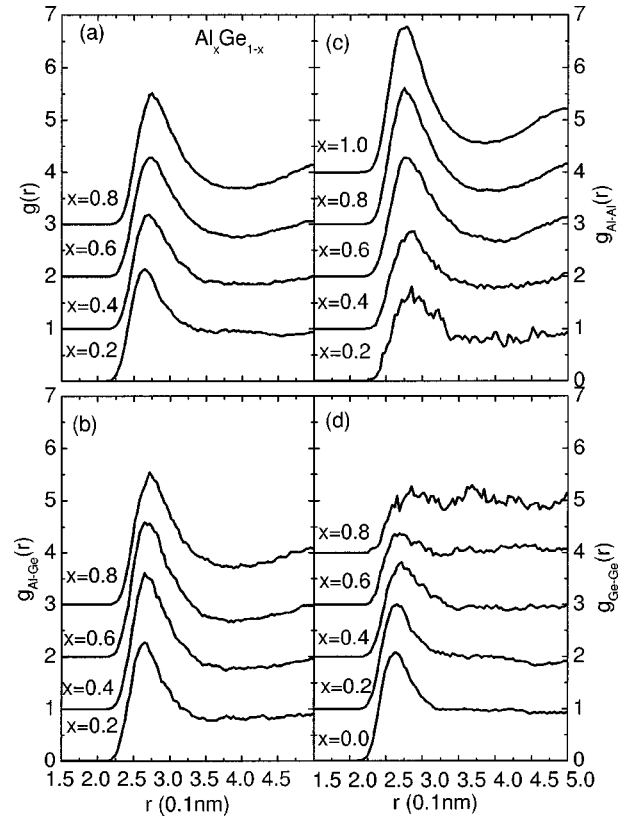
FIG. 1. Pair-correlation functions of Al$_x$Ge$_{1-x}$ at the temperature of 1250 K. (a) Total pair-correlation function; (b) partial pair-correlation function for Al-Ge; (c) partial pair-correlation function for Al-Al; (d) partial pair-correlation function for Ge-Ge. The graphs are vertically offset by one unit each for clarity.

The partial pair correlation functions between Ge and Al, $g_{\text{Al-Ge}}(r)$, at different Al concentrations, are shown in Fig. 1(b). The shapes of $g_{\text{Al-Ge}}(r)$ are similar to that of total $g(r)$ at the corresponding composition. The position of the first peak in $g_{\text{Al-Ge}}(r)$ shifts toward the larger value from 2.64 to 2.72 Å with increasing Al concentration. The height of the first peak in $g_{\text{Al-Ge}}(r)$ increases when the Al concentration x increases from 0.2 to 0.4, and remain almost unchanged when x increases to 0.6. When the concentration x is further increased to 0.8, the height of the first peak decrease to the value as that in the $x = 0.2$ sample. These results suggest that Al and Ge atoms are well mixed in the liquid phase. The partial pair correlation function between the Al atoms, $g_{\text{Al-Al}}(r)$ for four alloy compositions and pure liquid Al ($x = 1.0$) are shown in Fig. 1(c). The height of the principal peak of $g_{\text{Al-Al}}(r)$ increases with increasing the concentration of Al. In the sample of $x = 0.2$ Al concentration, the statistics for the $g_{\text{Al-Al}}(r)$ is poor because the number of Al atoms is too small. For $x = 0.8$, the position of the peak is almost the same as that of pure Al, i.e., at 2.74 Å. The partial pair correlation functions for Ge atoms, $g_{\text{Ge-Ge}}(r)$, at the different concentrations are shown in Fig. 1(d). The peak position ($r = 2.61$ Å) is not sensitive to the Al concentrations for $x < 0.6$ and is similar to that of the pure liquid Ge. It is interesting to note that at $x = 0.8$ there is a strong second peak at $\sim$3.66 Å, suggesting different ordering structures among the Ge atoms in the liq-
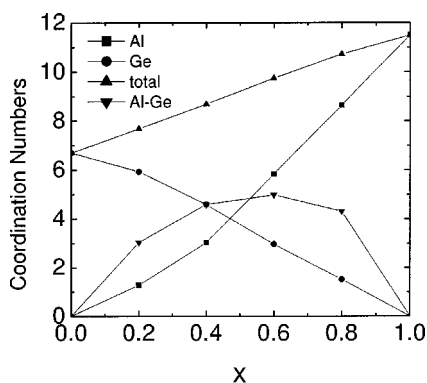
FIG. 2. Calculated coordination numbers as a function of Al concentration.

uid at this composition although the statistics is not very good due to the small number of Ge atoms in this sample.

By using the total and partial correlation functions, one can calculate the coordination numbers which are defined by

$$N_{ij} = \int_0^{R_{\min}} 4\pi r^2 g_{ij}(r)\rho_{ij}dr, \qquad (3)$$

where ρ_{ij} is the partial number density as defined in the first paragraph of this section. Figure 2 shows the total and partial coordination number as a function of Al concentration x in the liquid alloys. The cutoff of bond length $R_{\min}$ in Eq. (3) is taken to be 3.35 Å for Ge-Ge, 3.77 Å for Al-Al, and a linear interpolation value for Al-Ge according to their concentrations in the Al$_x$Ge$_{1-x}$ alloy. These values for $R_{\min}$ are very close to the corresponding first minimum of $g_{ij}(r)$. The N_{ij} gives the average number of j-type neighbor for an i-type atom within the first coordination shell in $g_{ij}(r)$. The average number of neighbors for Al$_x$Ge$_{1-x}$ alloys in the first shell is in the range 6.7–11.5 and increase with increasing the Al concentration. $N_{\text{Al-Al}}$ increases in a linear functions of Al concentration and $N_{\text{Ge-Ge}}$ decrease with increasing the Al concentration. Maximum coordination number $N_{\text{Al-Ge}}$ occurs when the Al concentration is about 50%.

The information about the short-range order in the liquid alloy may also be obtained from bond angle distribution functions $g_{ijk}(\theta)$. This function is defined for angles between nearest neighbors atoms around a central atom with a maximum bond length r_c. Namely, we consider a group of three atoms, one is denoted as the central atom (j), the other two atoms (i, k) denoted as side atoms, and a bond angle θ can be defined by these three atoms. $g_{ijk}(\theta)$ is the distribution of the bond angles formed by all such groups of three atoms with both the side atoms lie within a cutoff distance r_c from the central atom. The total $g_{\text{total}}(\theta)$ equals to the sum of all the partial $g_{ijk}(\theta)$. The bond length cutoff is the same as that used in the calculation of coordination numbers as discussed earlier. Figures 3 and 4 show the partial and total bond-angle distribution functions for the liquid Al$_x$Ge$_{1-x}$ alloys. The partial bond-angle distribution functions, $g_{\text{Al-Al-Al}}(\theta)$, $g_{\text{Ge-Al-Al}}(\theta)$, $g_{\text{Ge-Al-Ge}}(\theta)$, $g_{\text{Ge-Ge-Ge}}(\theta)$, $g_{\text{Ge-Ge-Al}}(\theta)$, and $g_{\text{Al-Ge-Al}}(\theta)$, are shown in Figs. 3(a)–3(f). $g_{\text{Al-Al-Al}}(\theta)$ has two peaks, one is around 56.5°, the others is around 106.5°. The
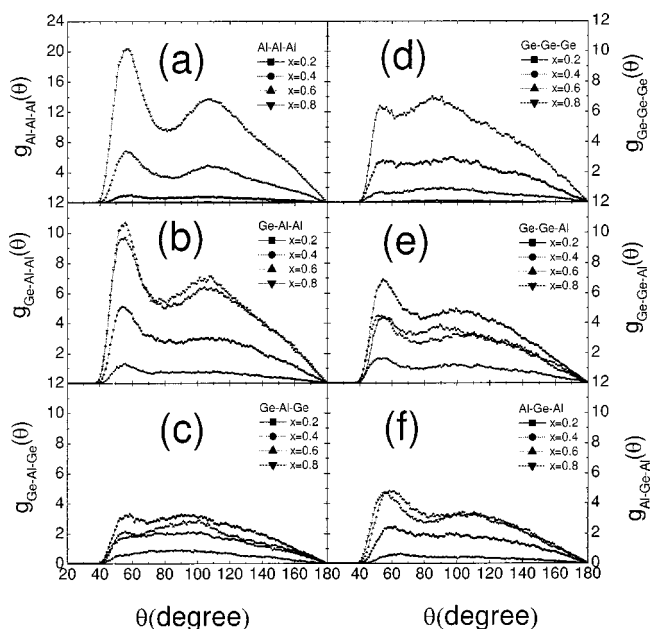
FIG. 3. Partial bond-angle distribution functions of liquid Al$_x$Ge$_{1-x}$ at 1250 K. (a) $g_{\text{Al-Al-Al}}(\theta)$, (b) $g_{\text{Ge-Al-Al}}(\theta)$, (c) $g_{\text{Ge-Al-Ge}}(\theta)$, (d) $g_{\text{Ge-Ge-Ge}}(\theta)$, (e) $g_{\text{Ge-Ge-Al}}(\theta)$, (f) $g_{\text{Al-Ge-Al}}(\theta)$.

height of the two peaks increases with increasing the Al concentration. $g_{\text{Ge-Ge-Ge}}(\theta)$ exhibits first peak around 55° and second peak around 89°, but the height of the first peak is lower than that of the second. Intermixing between Al and Ge can be seen from the mixed angle distribution functions $g_{\text{Ge-Al-Al}}(\theta)$, $g_{\text{Ge-Al-Ge}}(\theta)$, $g_{\text{Ge-Ge-Al}}(\theta)$, and $g_{\text{Al-Ge-Al}}(\theta)$, particularly in the samples of $x=0.4$ and 0.6. The total bond-angle distribution function shows two peaks. The first peak position shifts from 56.0° (for pure liquid Ge) to 56.8° (for pure liquid Al) with increasing the Al concentration. The second peak is broader and not as pronounce as the first ones for lower Al concentration, but it becomes more and more visible as the Al concentration increase. The second peak can also be seen to shift from about 90° to around 110° as the Al concentration is increased. It can be seen that the profile of the total bond-angle function is dominant by the partial bond-angle function of $g_{\text{Al-Al-Al}}(\theta)$.
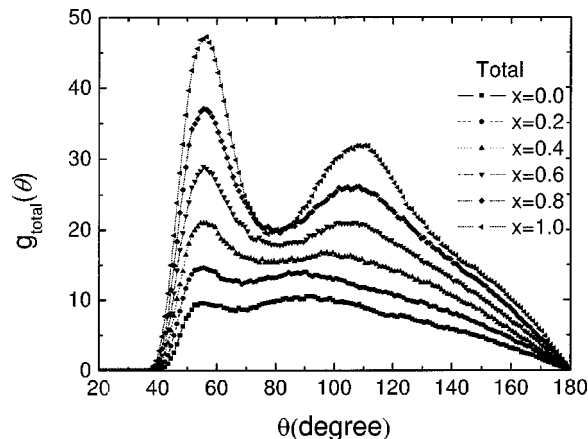
FIG. 4. Total bond-angle distribution functions of liquid Al$_x$Ge$_{1-x}$ at 1250 K.

The quantity which is commonly measured by experiment for liquid is the total structure factor $S(k)$. Experimental probes can only measure the total structure factor $S(k)$, but cannot directly separate the contributions of the partial components. From molecular dynamics simulation, it is possible to find the partial pair-correlation functions and partial structure factors. If we know the appropriate scattering parameters for each element in the liquid alloy, we can compare calculation results with neutron or x-ray scattering experiments.

In theoretical calculation, total structure factor $S(k)$ can be obtained by Faber-Ziman formalism[17] using the results of three partial structure factor $S_{ij}(k)$, the scattering lengths, and concentration of the elements in the alloys

$$S(k) - 1 = \frac{c_i^2 b_i^2 [S_{ii}(k) - 1] + 2c_i c_j b_i b_j S_{ij}(k) + c_j^2 b_j^2 [S_{jj}(k) - 1]}{c_i b_i^2 + c_j b_j^2},$$
(4)

where scattering lengths are $b_{Al} = 3.449$ and $b_{Ge} = 8.184$ for Al and Ge,[18] respectively. The Faber-Ziman partial structure factors,[19] $S_{ij}(k)$, are related to the partial pair correlation functions $g_{ij}(r)$ by

$$S_{ij}(k) = \delta_{ij} + 4\pi\rho_{ij} \int_0^\infty [g_{ij}(r) - 1] \frac{\sin(kr)}{kr} r^2 dr,$$
(5)

where i and j denote the two components of the binary alloy.

The total structure factor obtained from our calculations are compared with the results from experiments[8,10] as shown in Fig. 5(a). The peaks position matches very well with experimental results, but for the first peak height, there is a small discrepancy for high Al concentrations. Despite this difference, the overall agreement between the theory and experiment structure factors is good. Note that the partial structure factors for the like pairs [Figs. 5(c) and 5(d)] close to unity for k bigger than 6 Å^{-1}, while the structure factor between opposite pairs [Fig. 5(b)] is negative at small k and approaches zero for k bigger than 6 Å^{-1}. The peak in $S_{Al-Ge}(k)$ is higher in medium Al concentration as compare to that in low and high Al concentration.

The total pair correlation function, $g(r)$, can also be calculated by the Fourier transformation of $S(k)$ spectrum using the standard transformation techniques

$$g(r) = 1 + \frac{1}{2\pi^2 \rho r} \int_0^{k_{max}} k[S(k) - 1]\sin(kr) dk.$$
(6)

The total pair correlation functions calculated from Eq. (6) and the experimental results from Ref. 10 are compared in Fig. 6. The agreement between our calculated $g(r)$ and the experimental results are quite good. In both theoretical and experimental results, the peak position of $g(r)$ is shifted to positive direction from 2.66 to 2.76 Å with increasing the Al concentration. The peak heights obtained from our simulations are also similar to the experimental results and increase with increasing the Al concentration. Note that the peak height in the Fig. 6 is lower than that in Fig. 1(a) because the effects of the different scattering lengths for Al and Ge con-
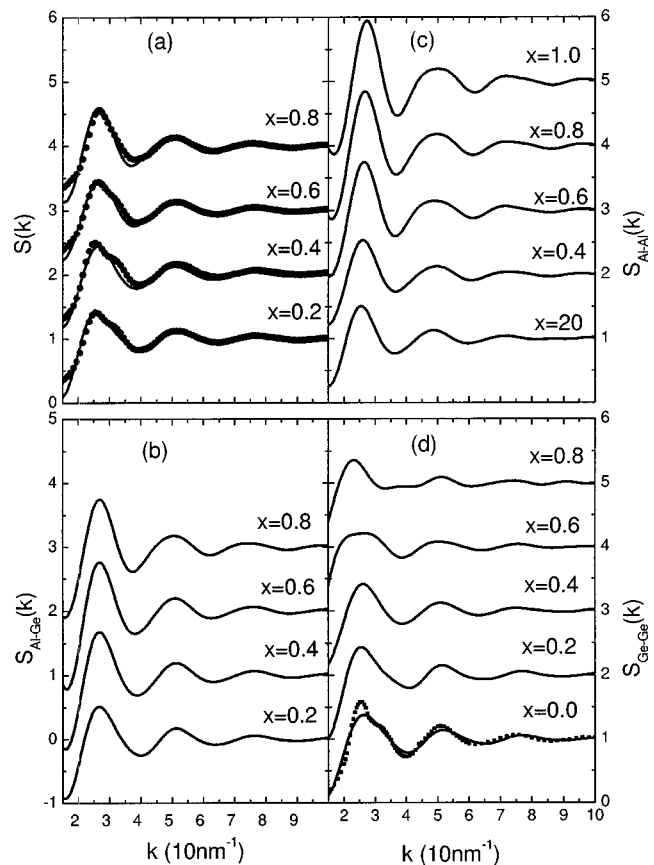
FIG. 5. Structure factors of Al_xGe_{1-x} at 1250 K. (a) Total structure factor; (b) partial structure factor of Al-Ge; (c) partial structure factor of Al-Al; (d) partial structure factor of Ge-Ge. The thin line: *ab initio*; dotted line: experiment. All the graphs are vertically offset one unit for clarity.

sidered in Fig. 6 are not included in the calculation for Fig. 1(a). For comparing $g(r)$ with experimental results, it is correct to include the effects of the scattering lengths. This requires experimental knowledge of the partial structure fac-
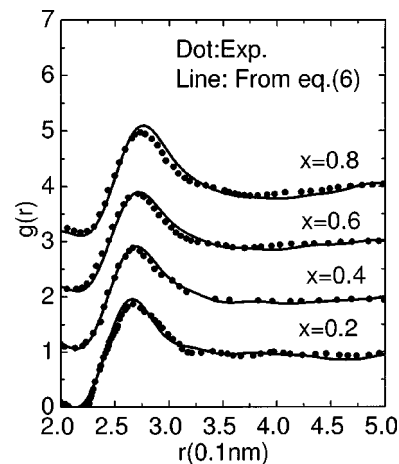
FIG. 6. Total pair-correlation functions for Al_xGe_{1-x} at temperature of 1250 K obtained from the simulations are compared with experimental data. The graphs are vertically offset by one unit each for clarity.
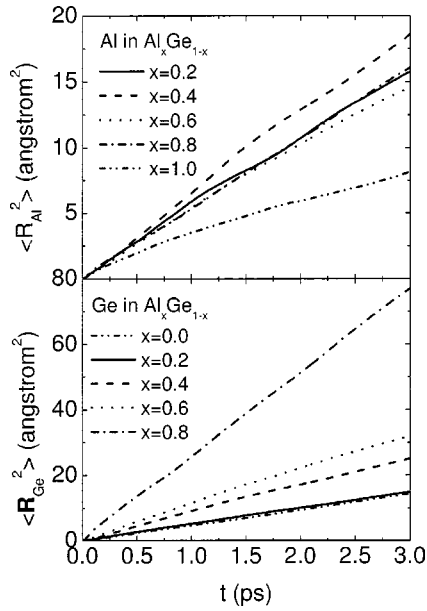
FIG. 7. Mean-square atomic displacement vs time t in liquid Al_xGe_{1-x} at 1250 K.

tors $S_{ij}(k)$, which cannot be determined from a single scattering experiment.

B. Dynamic properties

The dynamical properties of liquid Al_xGe_{1-x} have been investigated by calculating the atomic mean square displacement as a function of time

$$\langle R_\alpha^2(t)\rangle = \frac{1}{N_\alpha}\left\langle \sum_{i=1}^{N_\alpha} |\mathbf{R}_{ia}(t+\tau) - \mathbf{R}_{i\alpha}(\tau)|^2 \right\rangle, \qquad (7)$$

where N_α is the total atomic number of α species, $\mathbf{R}_{i\alpha}(t)$ is the coordinates of the ith atom, τ is the arbitrary origin of time. The average is taken for all possible τ. The results of $\langle R_\alpha^2(t)\rangle$ for the two components as a function of time t are plotted in Fig. 7. By using the Einstein relation, the self-diffusion constant D_{ii} can be estimated

$$D_{ii} = \lim_{t\to\infty} \langle R_{i\alpha}^2(t)\rangle/6t. \qquad (8)$$

The results for both types of atom are shown in Fig. 8. For pure Al and Ge liquids at 1250 K, the self-diffusion constant obtained from our simulations is 0.35×10^{-4} cm^2/s and 0.82×10^{-4} cm^2/s, respectively. The diffusion constant of pure liquid Al from our simulation is in the same order of magnitude but slightly smaller than the previous theoretical results of 0.49–1.05×10^{-4} cm^2/s (the temperature is in the range of 943–1323 K).[20] For liquid Ge, our result is in the range of previous theoretical results of 0.44–1.21 $\times10^{-4}$ cm^2/s at the temperature of 1250 K.[21] From our simulation results as plotted in Figs. 7 and 8, it can be seen that the self-diffusion constant for Al and Ge are not a linear function of Al concentration. The same feature has been observed in liquid Ag_xIn_{1-x} alloys.[22] An oscillating behavior is seen in the diffusion coefficients for Al, but the diffusion
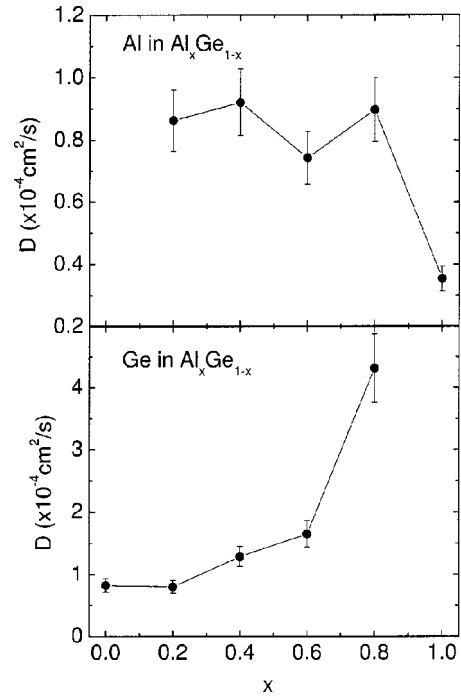
FIG. 8. Self-diffusion constant and its error bars for Al and Ge atoms in liquid Al_xGe_{1-x} at 1250 K.

coefficients for Ge increases with increasing the Al concentration. The oscillating behavior in the diffusion coefficients of Al may be due to the uncertainty in the calculations, mainly due to the uncertainty in choosing the density for the simulations as discussed in Sec. II. We first estimate the error bar in the diffusion coefficients for $Al_{0.6}Ge_{0.4}$ liquid alloy by performing the simulations for three different densities (i.e., 0.048 82, 0.049 33, 0.049 84 atom/Å^3, where 0.049 33 is the value from linear combination scheme). The error bars at other concentrations are then estimated using the same percentages from the error bar of the $Al_{0.6}Ge_{0.4}$ liquid alloy. These error bars are also plotted in Fig. 8. It can be seen that the oscillating behavior in the diffusion coefficients of Al are within the error bars. Therefore, the diffusion coefficient of Al in liquid Al_xGe_{1-x} alloys is almost a constant but it is about twice of the diffusion coefficient in pure liquid Al.

C. Electronic properties

The electronic density-of-states (DOS) of liquid Al_xGe_{1-x} are calculated from the expression

$$N(E) = \sum_{k,E_k} w_k g(E - E_k), \qquad (9)$$

where E_k is the eigenvalues of the one-electron Hamiltonian at a particular k point of the supercell Brillouin zone and w_k is the weight of that k point. $g(E)$ is a Gaussian function with a width of 1.0 eV. The set of eight special k points in the supercell Brillouin zone, i.e, $\left(\frac{1}{8},\frac{1}{8},\frac{1}{8}\right)$, $\left(\frac{1}{8},\frac{1}{8},\frac{3}{8}\right)$, $\left(\frac{1}{8},\frac{3}{8},\frac{1}{8}\right)$, $\left(\frac{3}{8},\frac{1}{8},\frac{1}{8}\right)$, $\left(\frac{1}{8},\frac{3}{8},\frac{3}{8}\right)$, $\left(\frac{3}{8},\frac{3}{8},\frac{1}{8}\right)$, $\left(\frac{3}{8},\frac{1}{8},\frac{3}{8}\right)$, $\left(\frac{3}{8},\frac{3}{8},\frac{3}{8}\right)$ used by Holender[2] is used in the present calculation. Each k point has the same weights w_k. For each k point we chose lowest 150
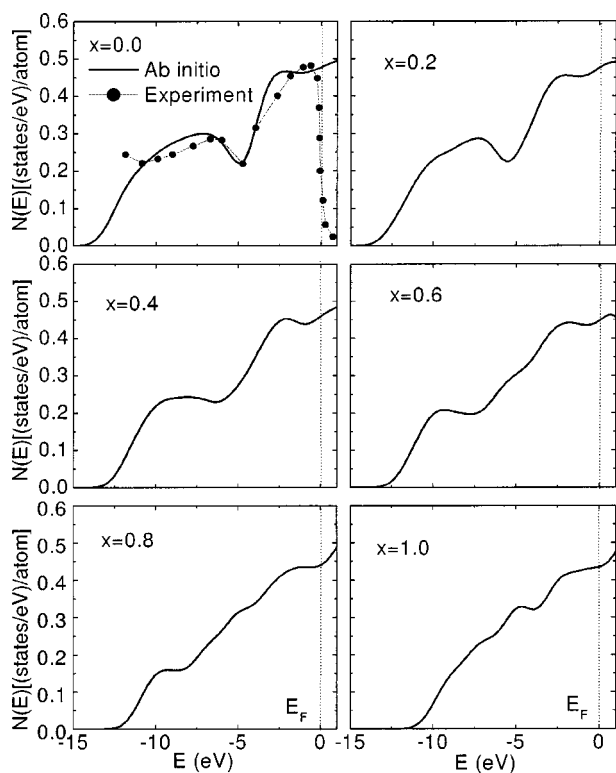
FIG. 9. Calculated electronic density of state $N(E)$ for liquid Al_xGe_{1-x} at the temperature of 1250 K.

eigenvalues E_k, and the final density-of-states are then obtained by averaging over 15 representative configurations for each concentration. The Fermi energy is shifted to zero for the presentation.

The calculation results are shown in Fig. 9 for the four concentrations of Al_xGe_{1-x} alloys and the pure Al and Ge at the same temperature of 1250 K. The calculated DOS of liquid Ge is in good agreement with the measured photoemission intensities.[23] A pseudogap at 4.6 eV is presented in the liquid Ge. It has been shown[24] that the formation of the pseudogap is due to an increasing s-p splitting arising from the relativistic effect for Ge. Unlike the Ge, the DOS of liquid Al has the free electron like behavior. From Fig. 9, it can be seen that when the system changes from pure liquid

Ge to pure liquid Al, the pseudogap in the DOS is filled up as the Al concentration increase, and its position is shifted to lower energies relative to Fermi energy. The pseudogap becomes hardly visible at the concentration $x=0.8$. It is also interesting to note that there is a minimum in the DOS close to (although not exactly at) the Fermi level in the liquid Al_xGe_{1-x} alloy. This minimum is more pronounce when $x=0.4$ and 0.6. This feature is also consistent with the experimental results of photoelectron spectroscopy.[12]

IV. CONCLUSIONS

In conclusion, we have carried out *ab initio* molecular dynamics simulations for liquid Al_xGe_{1-x} alloys at four different concentrations at a temperature of 1250 K. The total coordination number increased in a linear function with the concentration of Al. The first peak positions of the total pair correlation function and structure factor shift toward larger values with increasing the concentration of Al. Our results of pair-correlation functions and structure factors are in good agreement with the available experimental data. Our simulation results also show that the diffusion coefficients of Al and Ge in liquid Al_xGe_{1-x} alloys are larger than that in the corresponding pure liquids. The electronic DOS of the liquid Al_xGe_{1-x} alloys changes from the heavier liquid group-IV element to the free-electron like as the Al concentration increases.

[1] G. Kresse and J. Hafner, Phys. Rev. B **49**, 14 251 (1994).

[2] J. M. Holender, M. J. Gillan, M. C. Payne, and A. Simpson, Phys. Rev. B **52**, 967 (1995).

[3] F. Kirchhoff, J. M. Holender, and M. J. Gillan, Phys. Rev. B **54**, 190 (1996).

[4] R. V. Kulkarni and D. Stroud, Phys. Rev. B **62**, 4991 (2000).

[5] R. V. Kulkarni and D. Stroud, Phys. Rev. B **57**, 10 476 (1998).

[6] L. Vočadlo, D. Alfè, G. D. Price, and M. J. Gillan, Phys. Earth Planet. Inter. **120**, 145 (2000).

[7] C. Massobrio, A. Pasquarello, and R. Car, Phys. Rev. B **64**, 144205 (2001).

[8] http://www.iamp.tohoku.ac.jp/database/scm/LIQ/sq.html

[9] Y. Waseda, *The Structure of Non-Crystalline Materials* (McGraw Hill, New York, 1980).

[10] B. Grosdidier and J. G. Gasser, J. Non-Cryst. Solids **250–252**, 309 (1999); (private communication).

[11] B. Grosdidier and J. G. Gasser, Intermetallics **11**, 1253 (2003).

[12] R. Gampp, F. Baumann, H. G. Boyen, A. Cossy-Favre, G. Gantner, P. Oelhafe, and P. Häussler, J. Non-Cryst. Solids **156–158**, 236 (1993).

[13] G. Kresse and J. Hafner, Phys. Rev. B **47**, 558 (1993); G. Kresse, Ph.D. Technische Universität Wien, 1993; G. Kresse and J. Furthmüller, Comput. Mater. Sci. **6**, 15 (1996); G. Kresse and J. Furthmüller, Phys. Rev. B **54**, 11 169 (1996).

[14] A. F. Crawley, Int. Metall. Rev. **19**, 32 (1974).

[15] S. Nosé, J. Chem. Phys. **81**, 511 (1984); W. G. Hoover, Phys. Rev. A **31**, 1695 (1985).

[16] G. Kresse and J. Joubert, Phys. Rev. B **59**, 1758 (1999).

[17] T. E. Faber, *An Introduction to the Theory of Liquid Metals* (Cambridge University Press, Cambridge, 1972).

[18] National Nuclear Data Center at Brookhaven National Lab, Neutron News **3**, 29 (1992).

[19] P. A. Egelstaff, *An Introduction to Liquid State*, 2nd ed. (Calrendon, Oxford, 1994), Appendix 4.

[20] D. J. González, L. E. González, J. M. López, and M. J. Stott, Phys. Rev. B **65**, 184201 (2002).

[21] R. V. Kulkarni, W. G. Aulbur, and D. Stroud, Phys. Rev. B **55**, 6896 (1997).

[22] M. I. Mendelev, J. Non-Cryst. Solids **232**, 560 (1999).

[23] G. Indlekofer, P. Oelhafen, R. Lapka, and H. J. Güntherodt, Z. Phys. Chem. (Munich) **157**, 465 (1988).

[24] W. Jank and J. Hafner, Phys. Rev. B **41**, 1497 (1990).